CHAPTER 3 DESIGN OF A SPMB AND FREE FLAME TEST

3.1 Design of SPMB

A design criterion of the SPMB is relied on the characteristics of the CB such as with an equal pressure drop ΔP across the burner ports to preserve the same primary aeration and with almost an equal net port area for desirable flame stabilization. The SPMB is formed by a vertical packed bed of spherical particles of alumina spheres, below which is connected with a mixing chamber. An alumina sphere diameter, d, and an exit area of the mixing chamber are very important for flame stabilization and combustion characteristics. An alumina sphere diameter d is estimated by using a modified Pe [38] as shown by Eq. (3.1).

$$Pe = \frac{S_L d c_p \rho}{k} \tag{3.1}$$

If $Pe > 65$, a flame can propagate and stabilize within the packed bed. On the other hand, the flame can not propagate within the packed bed if $Pe < 65$ because of quenching. Heat is transferred to the packed bed at a higher rate than it is produced. To obtain desirable flame stabilization within the packed bed and favorable combustion characteristics, the SPMB has to be designed based on $Pe > 65$.

Pressure drop ΔP across the packed bed of the SPMB can be estimated by means of an empirical formula of Ergun [39] as shown by Eq. (3.2).

$$\frac{\Delta P}{L} = aU + b^2 U^2 \tag{3.2}$$

where

$$a = 150 \frac{\mu}{d^2} \frac{(1-\varepsilon)^2}{\varepsilon^3} \tag{3.3}$$

$$b = \sqrt{1.75 \frac{\rho}{d} \left(\frac{1-\varepsilon}{\varepsilon^3} \right)} \tag{3.4}$$

$$U = \frac{Q}{A} \tag{3.5}$$

$$\varepsilon = 0.4 + 0.01\left[\exp\left(\frac{10.686}{(D_p/d)}\right) - 1\right] \tag{3.6}$$

Here, ΔP is an assigned value from the CB experiment and is a function of the volume flow rate of the mixture Q or the firing rate CL. Therefore, various configurations of the SPMB having a specified pressure drop across the burner of ΔP can be formed depending on the combination of the pertaining parameters of alumina sphere diameter d and the packed bed diameter D_p. Once the alumina sphere diameter d and the packed bed diameter D_p are selected, a packed bed void fraction ε can be estimated from the empirical expression of Zou and Yu [40] as shown by Eq. (3.6). The constant parameters a and b in Eqs. (3.3) and (3.4), respectively, can then be calculated with the known void fraction ε. Therefore, the packed bed length L of the SPMB can be estimated from Eq. (3.2) as a function of ΔP and superficial velocity U as shown by Eq. (3.5), which is proportional to the volume flow rate of the mixture Q or the firing rate CL.

Figure 3.1 shows the variation of the interstitial velocity V and the packed bed length L with the firing rate CL at $D_p = 0.15$ m and $d = 0.015$ m. The interstitial velocity V is obtained by using Eq. (3.7).

$$V_p = \frac{U}{\varepsilon} \tag{3.7}$$

The result shows that the calculated interstitial velocity V_p is slightly higher than the corresponding laminar flame speed S_L [18] by a factor of 1.15. This is done to compensate for an increase in value of the actual laminar flame speed S_L within the packed bed owing to an internal heat recirculation from the hot products to the cool reactants. At maximum firing rate of $CL = 70$ kW, the corresponding length $L = 0.15$ to 0.17 m of the packed bed is seemed to be sufficient for flame stabilization within the packed bed while retaining the primary air entrainment with the same pressure drop ΔP as those that occurred in the CB. An initial 3-D design of the SPMB as shown in figure 3.2.

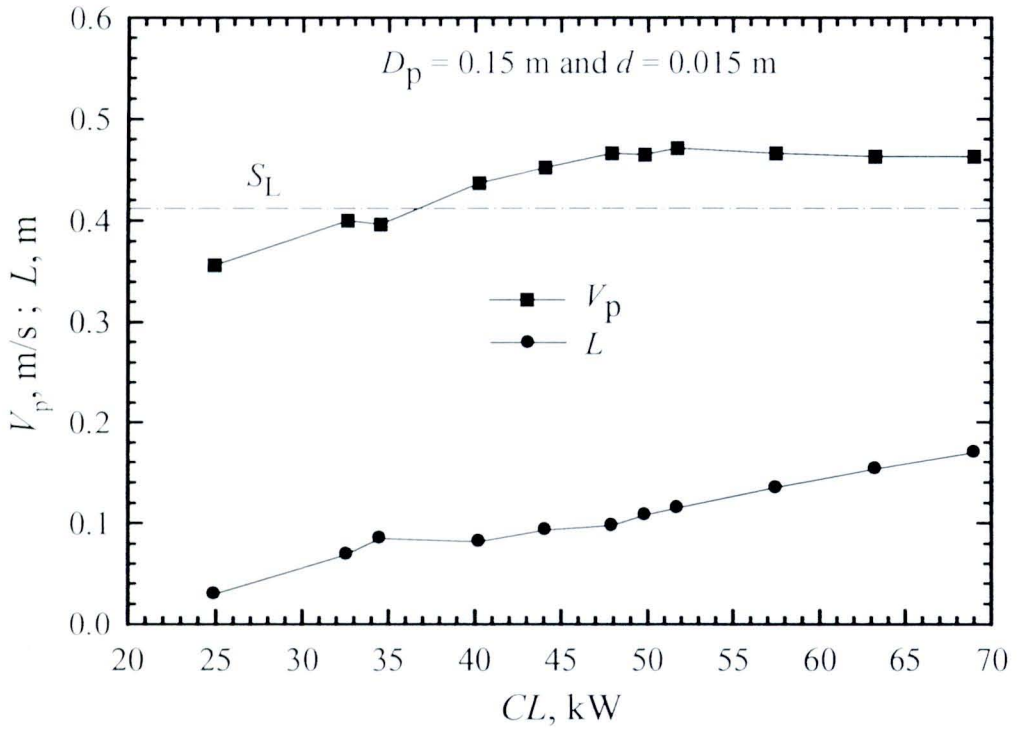

Figure 3.1 A relationship between CL and L and V_p.

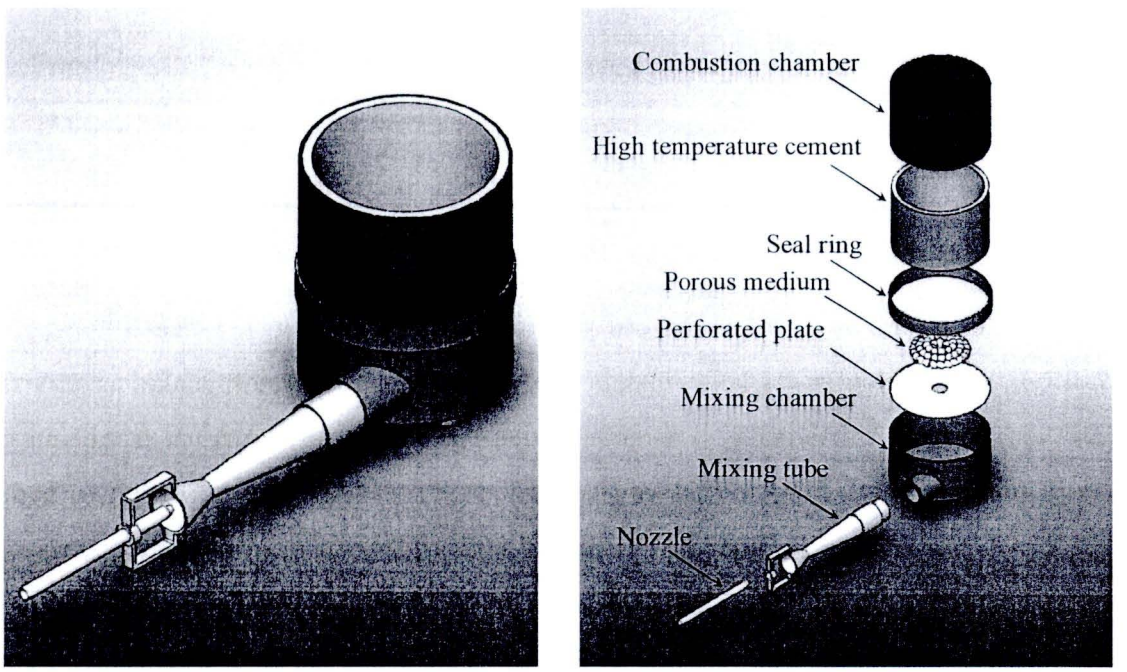

Figure 3.2 Initial 3-D design of the SPMB.

3.2 Setup and preliminary test

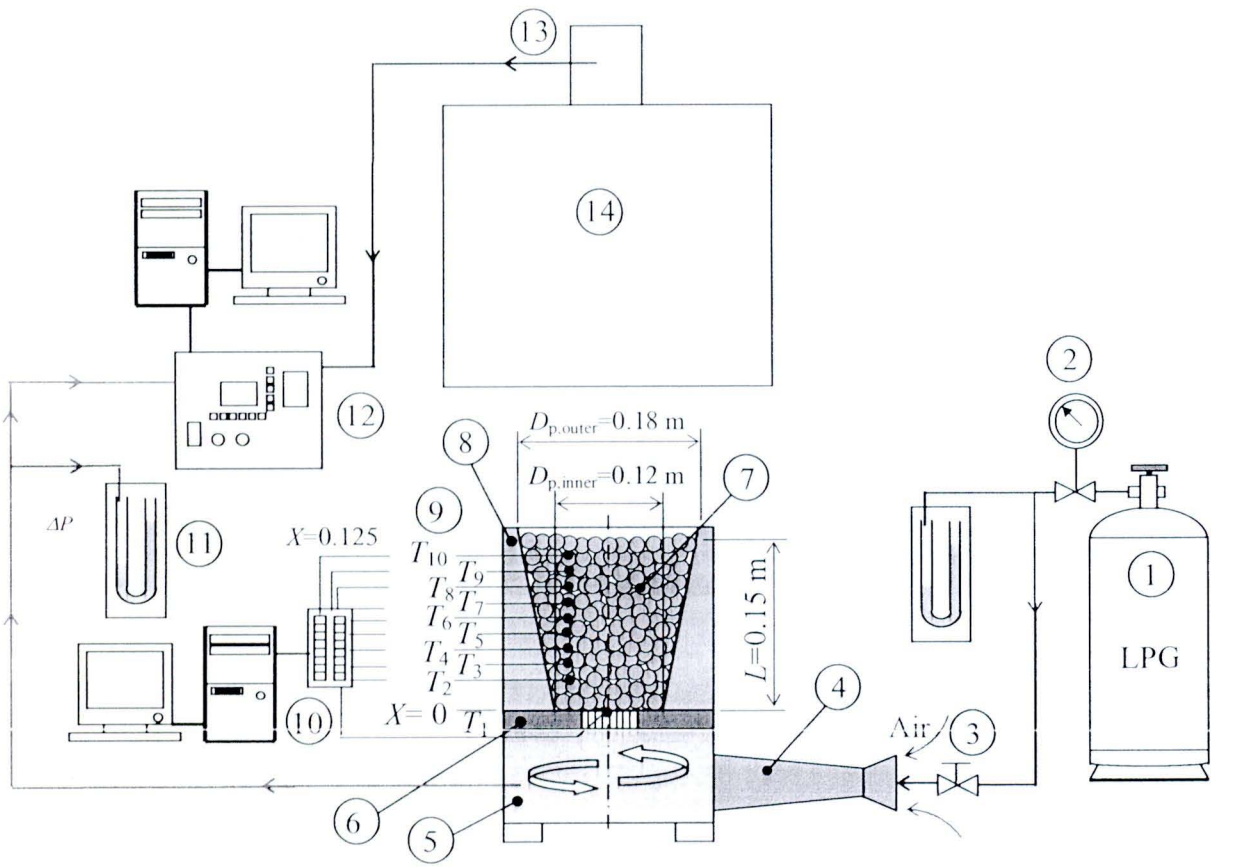

1. Fuel (LPG); 2. Pressure gauge and mercury manometer; 3. Ball valve; 4. Mixing tube; 5. Mixing chamber; 6. Perforated stainless steel plate; 7. Packed bed; 8.High temperature cement; 9. Thermocouples; 10. Data logger; 11.Water manometer; 12. Exhaust gas analyzer and oxygen sensor; 13. Probe; 14. Hood

Figure 3.3 Schematic diagram of the experiment setup of SPMB.

Figure 3.3 shows a schematic diagram of the experimental setup for SPMB, whereas figure 3.4 shows a thermocouple setting and outside details of the SPMB. The SPMB comprises four main parts: a mixing tube (4), a mixing chamber (5), a perforated steel plate (6) and a packed bed (7). The mixing tube (4) is made of a cast iron and is tangentially connected with the mixing chamber (5), which is made from a cylindrical steel tube having inside diameter of 0.2 m and wall thickness of 3 mm. The packed bed of the SPMB (7) is formed by a randomly arranged alumina spheres with particle diameter of d = 0.015 m placed inside an imaginary cylinder having a diameter and height of equal value of 0.15 m. To increase a heat transfer area for thermal radiation emitted to downstream side of the packed bed, the imaginary cylindrical packed bed

obtained from the calculation is transformed into a conical shape with average diameter equivalent to that of the cylindrical one of D_p = 0.15 m. The packed bed (7) is surrounded by a high temperature cement (8) and is supported by the perforated stainless steel plate (6), which has the total flow area of about 2,015 mm^2 so as to allow for the incoming flow of the fuel/air mixture from the mixing chamber (5) to flow through the packed bed (7) and to be burned within the packed bed without flame flash back or blow-off phenomenon. Determination of the total flow area of the perforated stainless steel plate (6) depends on the CB's net port area and diameter of a fuel nozzle installed at the mixing tube inlet. The total flow area of the perforated stainless steel plate (6) should be kept equal or less than that of the CB's net port area so as to avoid the risk of flashback phenomenon of flame from propagating into the mixing tube (4). Assembly of the SPMB is shown in appendix D.

A LPG (1) is used as a fuel in the experiment. It contains 40 percent (by volume) of propane (C_3H_8) and 60 percent of butane (C_4H_{10}) with a low heating value of about 108 MJ/m^3 [normal]. The LPG flow rates are controlled by a pressure regulator with calibrated pressure gauge (2), mercury manometer and ball valve (3) that is connected with the fuel nozzle having diameter of 1.6 mm.

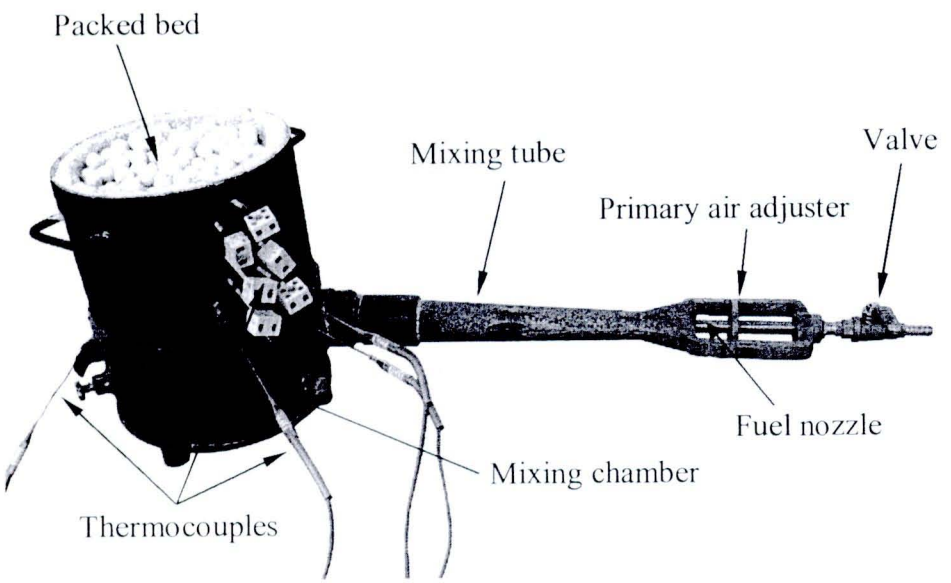

Figure 3.4 Photograph of the SPMB's details.

The temperatures within the packed bed are measured by setting 10 locations of thermocouples (9) with different types depending on location as denoted by T_1 to T_{10} as shown in figure 3.3. At $X = 0$, temperature T_1 locate at the center of the interface between the packed bed (7) and the perforated stainless steel plate (6) . Within the packed bed (7) where combustion takes place, the thermocouples are equidistantly located at T_2-T_{10} as shown in figure 3.3. The tips of these thermocouples are not placed on the centerline of the packed bed but at about 30 mm away from burner centerline. The temperatures at T_1 to T_4 are of N-type sheath thermocouples with 1.5 mm in diameters, whereas the temperatures at T_5 to T_{10} are B-type bare thermocouples (Pt/Pt-Rh 13 percent) with 0.5 mm in diameters. The signals of thermocouples are digitized by a general purpose data logger (10) (Delta model DT-600), and then transmitted to a personal computer.

The pressure drop across the packed bed (ΔP) of the SPMB is measured by a manometer (11) at the side wall of the mixing chamber (5) . Meanwhile the oxygen sensor (12) is used to measure oxygen concentration (O_2) within the mixture with an accuracy of about 0.05 percent. An uncertainty analysis of measured oxygen concentration (O_2) was carried out with the method proposed by Kline and McClintock [41]. Using a 95 percent confidence level, the maximum and minimum uncertainties in the presented primary aeration were found to be 4.7 percent relative and 2.2 percent relative, respectively. By using Eq. (3.8) [11], the primary aeration (PA) in the mixing tube (4) is estimated from the measured O_2 concentration to monitor quality of the mixture before combustion within the packed bed.

$$PA = \frac{\%O_2}{(A/F)_{stoi} \times (21 - \%O_2)} \times 100 \qquad (3.8)$$

Emission analysis of the dry air combustion products at the exit (13) of the hood (14) is carried out by using a portable exhaust analyzer (12) (Messtechnik Eheim model Visit01L). A gas processing system of CO and NO_x is especially tuned for electrochemical sensors, ensuring long-time stability and accuracy of measurement. The measuring range of the analyzer is 0 to 10,000 ppm for CO and 0 to 4,000 ppm for NO_x with a measuring accuracy of about ±5 ppm and a resolution of 1 ppm for both CO and NO_x. All measurements of emissions in the experiment are those corrected to 0 percent excess oxygen and dry-basis.

To start-up the SPMB, a diffusion free flame stabilized over the top surface of the packed bed (7) is established first before switching to a submerged partially premixed flame. The diffusion free flame is made by fully closing a primary air adjuster at the mixing tube inlet (see figure 3.4) and using a relatively low firing rate (CL) of about 23 kW. Then the primary air adjuster is gradually opened to allow for a more primary air being entrained into the mixing tube. This makes the flame being transformed into a more partially premixed one. At a certain value of opening of the primary air adjuster, the flame over the packed bed (7) automatically propagates into the packed bed. At this transient time, all temperatures are recorded for studying the evolution of temperatures within the packed bed. Once a steady state submerged premixed flame is established, the firing rate CL is increased to a desired value by increasing the LPG pressure with setting the primary air adjuster at a full opening position. Then, the temperature profiles within the packed bed and the emissions of CO and NO_x at the packed bed exit are measured by inserting a probe through the exit (13) of a hood (14) for collecting the exhaust gases.

3.3 Results of the SPMB's free flame

3.3.1 Evolution of temperature within the SPMB

Transient behavior of temperatures within the packed bed of SPMB during switching from a diffusion free flame stabilized over the surface of the packed bed to a steady state submerged partially premixed flame is a very interesting phenomenon. Figure 3.5 shows a typical transient changes of the solid phase temperatures T within the packed bed at an initial firing rate of CL = 23 kW. A cool mixture temperature at the inlet of the packed bed is represented by T_1 and is always constant without varying with time t. During $0 < t < 73$ s represents the burning time of the diffusion free flame stabilized over the surface of the packed bed. Reaction mainly takes place outside the packed bed with flame lifting over the packed bed surface. The flame is not felt up by the internal portion of the packed bed and thus, all temperatures within the packed bed are equal to an inlet temperature of the fresh mixture of T_1 = 34°C. At a certain opening of the primary air adjuster at about t = 73 s, the flame automatically propagates into the upstream side of the packed bed, resulting in an abrupt increase in T_2 at the position of X = 25 mm. This means that a submerged partially premixed flame is accomplished by utilizing a flashback phenomenon.

Once the first flame within the packed bed is appeared at the location of X = 25 mm where T_2 become maximum, the packed bed in the vicinity of that location is heated to a certain high temperature, which provides an important heat source for further ignition. However, the flame can not be stabilized at that location because of an imbalance between the burning velocity and the flow velocity of the fresh mixture. Then, the flame behaves a self-adjustment by moving to downstream of the packed bed and utilizing T_2 as a heat source for ignition until a new flame location of X = 37.5 mm is reached, where T_3 become maximum. This new flame location then provides a heat source for ignition of the next new flame location, and so on. Thus, the flame moves downstream with time t until a new flame location with maximum temperature appears at the location of T_8 at X = 100 mm, beyond which variation of the flame location remain unchanged and steady state combustion within the packed bed is established.

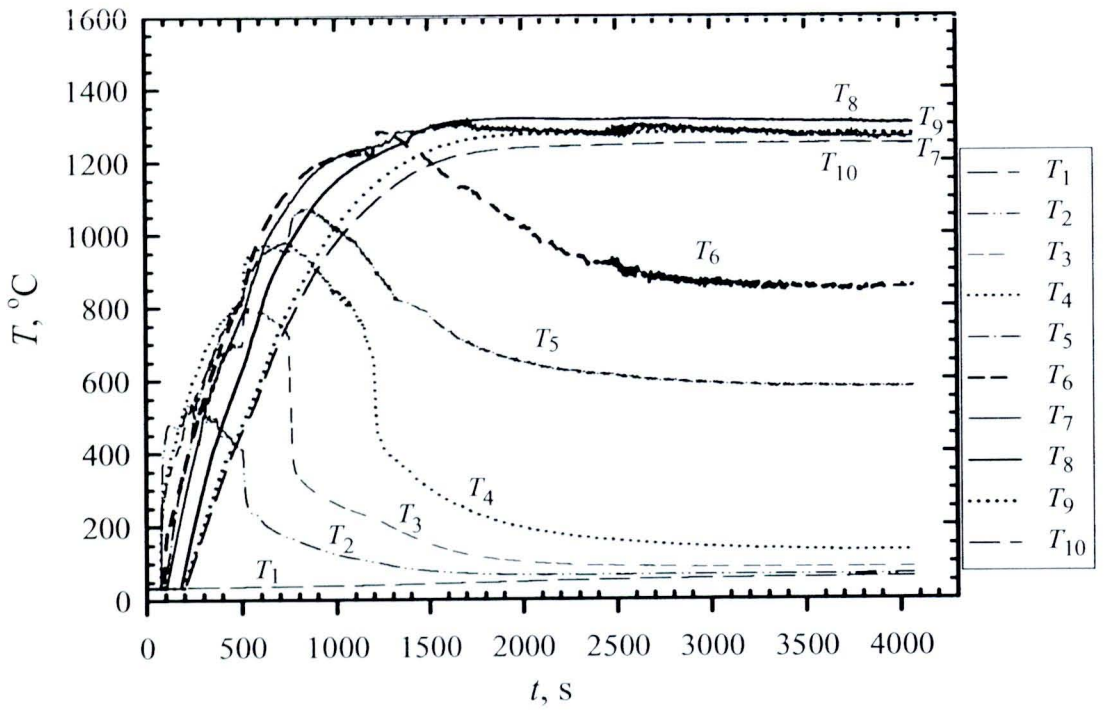

Figure 3.5 A history of SPMB's temperature.

3.3.2 Flame movement phenomenon

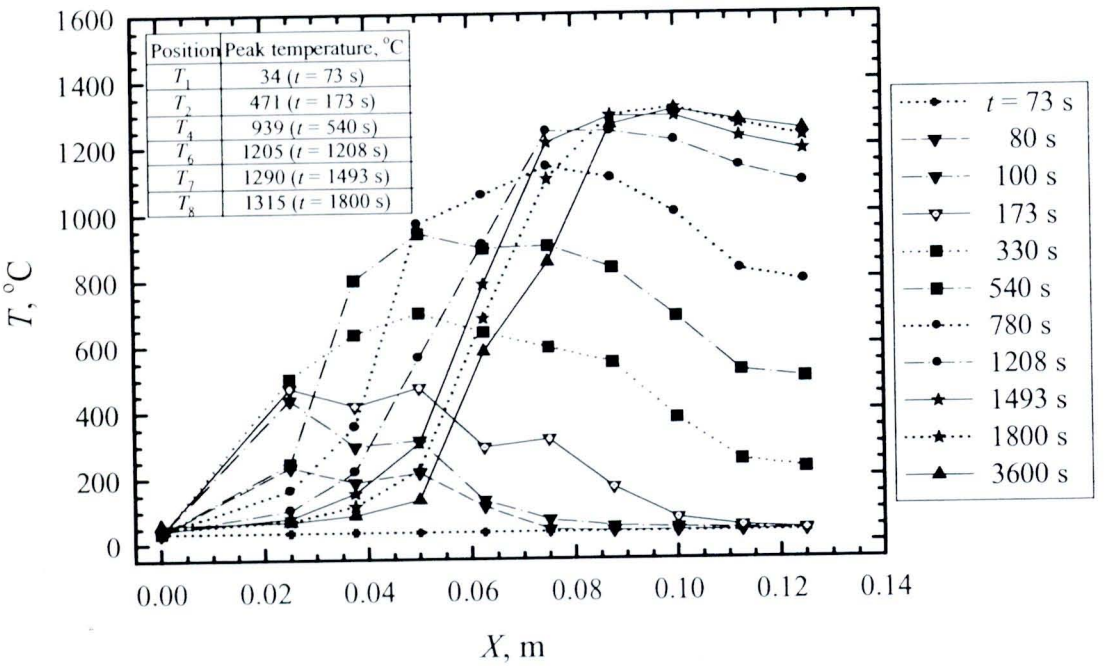

Figure 3.6 Transient temperature distributions along the length of the SPMB.

Flame movement phenomenon within the packed bed of the SPMB during the start-up period of the burner can be clearly understood by visualizing the corresponding transient temperature distributions along the axis X of the SPMB as shown in figure 3.6. At t = 73 s represents the time before the onset of the flash back phenomenon. All temperatures within the packed bed at this time are equal to the inlet temperature of the fresh mixture at T_1 = 34°C. At t = 80 s, the onset of the flash back phenomenon the internal portion deep within the packed bed at the region of X = 0.025 to 0.06 m is felt up by the combustion heat, implying an initial reaction taking place within the packed bed. As t increases, the temperatures within the packed bed further increase together with an expansion of the reaction zone to the downstream side of the packed bed. However, an increase in temperatures within the packed bed is accompanied by a shifting in the location of the maximum temperature to the downstream side of the packed bed, implying a flame movement. This flame movement is confirmed by a decrease in the temperature in the upstream side and an increase in temperature in the downstream side of the packed bed. At t = 3600 s, the flame eventually moves to a certain location of X = 0.1 m with maximum temperature of T_8 = 1315°C, beyond which

variation of the flame location remain unchanged with time t. Therefore, a steady state, fully submerged flame is established within the packed bed at the location of $X = 0.1$ m, which stays within the length of the packed bed $L = 0.15$ m. Therefore, about one-third of the packed bed length from above is in the glowing state like burning of the charcoal with an intense thermal radiation emitted from the top surface of the packed bed.

The transition period from initial diffusion free flame to final steady state submerged flame may requires 3600 s (about 1 hour), which is too long for household application because cooking may be finished within this time of period. However, the SPMB is designed to be used mainly in SMEs in Thailand for continuous food processing industry rather than for a daily cooking in a small family. Therefore, the process time in the food processing industries is far more than the transition period of the SPMB because the average working hour for the food processing industries are normally more than 8 hours a day. In fact, the transition period of the SPMB can be less than 3600 s. Based on figure 3.5, the burner may be ready and hot enough to transfer heat to a thermal load at the early time of $t = 1500$ s (25 min) because the flame has been stop propagating and is completely stabilized at the location of T_8 at $X = 0.1$ m. Further reduction in the transition period can be done by using relatively low thermal capacity and low density materials such as yttria-stabilized zirconia/alumina composites (YZA ceramic foam), which is scheduled to be done in the future work.

The obtained steady state temperature profile at $t = 3600$ s represent the solid phase (or packed bed) temperature because the thermocouples are also solid by themselves. Correction to the thermocouple reading will help to improve accuracy of the measured values closer to the true gas phase temperature. But this was not done because of several effects of heat transfer within the packed bed. However, the measured temperature can be used to describe the combustion phenomena within the packed bed. Based on the measured steady state temperature profile at $t = 3600$ s, it can be stated that the obtained temperature profile behaves much the same as that of the fully premixed flame stabilized within the porous matrix with steep temperature gradient at the pre-flame zone owing to a self-preheating characteristic of the packed bed. A small decrease in the post-flame zone temperature is also realized owing to heat losses to the downstream surrounding by intense thermal radiation and convection.

3.3.3 Effect of *CL* on temperature distribution

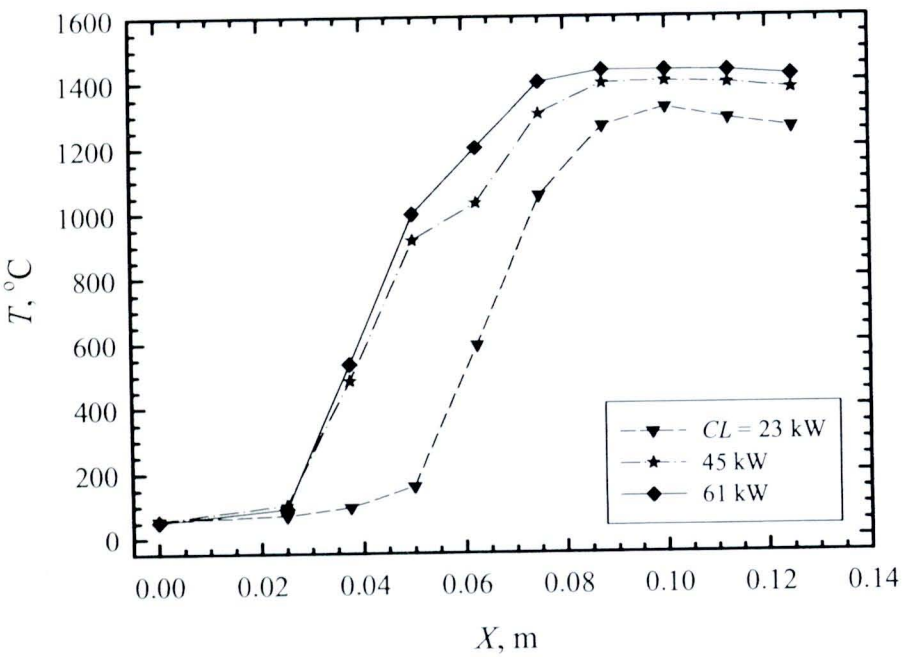

Figure 3.7 Effect of *CL* on steady state temperature distribution.

Figure 3.7 shows an effect of the firing rate *CL* on the steady state temperature profiles along the axis *X* of the packed bed at varying firing rate *CL* from 23 to 61 kW (all temperature profiles of SPMB's free flame is shown in figure B.3). Variation of the firing rate *CL* is obtained by varying the inlet pressure of the gaseous fuel at the fuel nozzle so as to study a turn-down ratio of the SPMB. The firing rate *CL* is considered as a dominant controlling parameter of the SPMB performance. At a relatively low firing rate of *CL* = 23 kW the location of the flame is at *X* = 0.1 m with the maximum temperature of about 1,315°C. As the firing rate is increased to *CL* = 45 kW, the flame shows a trend of moving to the upstream region because the preheating zone with steep temperature gradient is significantly shifted to the upstream region. Improvement in mixing caused by an increase in turbulence owing to the presence of the packed bed and an increase in the *PA* may contribute to this flame movement upstream. The flame temperature is significantly increased with the maximum temperature of about 1,400°C because of an increase in the heat content of the mixture. As the firing rate is increased to *CL* = 61 kW, the maximum temperature is increased to about 1,434°C without further flame movement to the upstream zone. For the range of *CL* studied in this experiment, the SPMB has a relatively high turn-down ratio of about 2.65, which is sufficient for the SMEs applications in Thailand.

3.3.4 Effect of *CL* on pressure drop and primary aeration

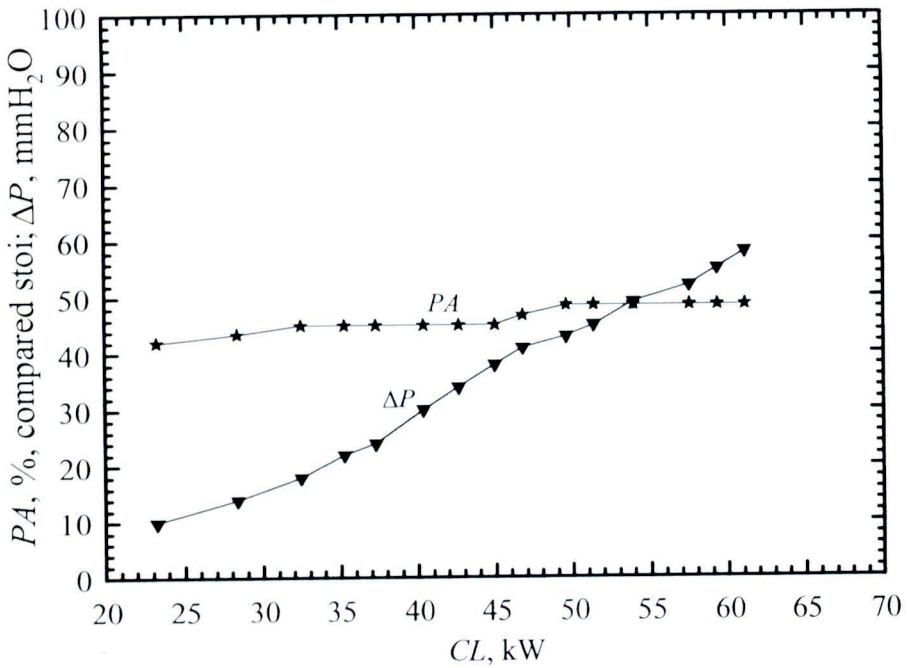

Figure 3.8 Effect of *CL* on ΔP and *PA*.

Figure 3.8 shows variations of the *PA* and the pressure drop ΔP with *CL* for SPMB. The measurement technique and estimation of the *PA* used by Namkhat and Jugjai [11] is adopted in this study. Within the range of *CL* studied, both *PA* and pressure drop ΔP are almost linearly increased with *CL* because of a fundamental phenomenon of the self-aspirating burner [42]. However, the *PA* of the SPMB has shown an asymptotic value as the *CL* is larger than 50 kW because the primary air entrainment is limited by the characteristic of the mixing tube [11, 42]. The measured *PA* is ranged from about 40 to 48 percent. This implies that the combustion taking place within the packed bed is operated within the fuel-rich flame regime, which is true for the self-aspirating burners. Therefore, the corresponding equivalence ratio is ranged from 2.08 to 2.50. Despite the fuel-rich combustion regime, the flame can be well stabilized within the packed bed because of the unique characteristic of the porous medium burner in enhancing the burning velocity of the mixture by a self-preheating effect through the interaction between the gas and the solid phases. The pressure drop across the packed bed ΔP for the SPMB is linearly increased with *CL*, which is well agreed with that of the CB because the overall design of the SPMB is based on the basic characteristics of the CB.

3.3.5 Emission characteristic of SPMB's free flame

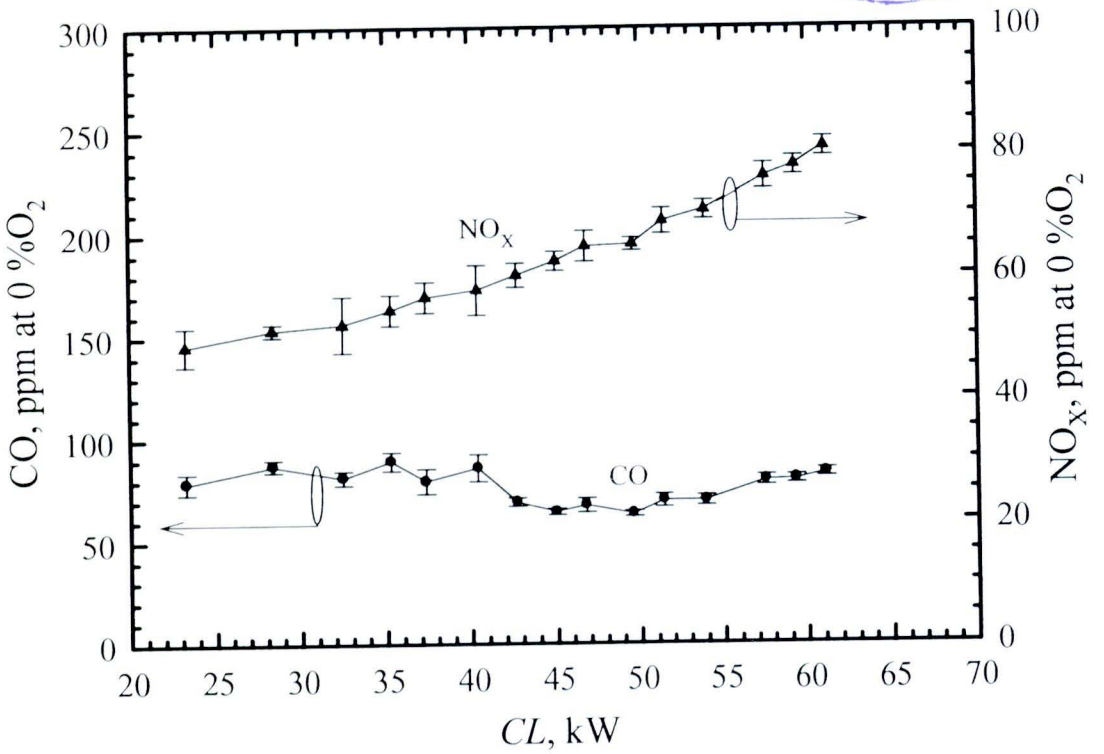

Figure 3.9 Emission of free flame of the SPMB.

Figure 3.9 shows effect of the firing rate *CL* on CO and NO_x emissions. Error bars show range or span, which is a difference in maximum and minimum values of the experimental data. The measured values of CO and NO_x do not reflex actual combustion characteristics within the packed bed since the sampling probe is not placed inside the packed bed but it is located at the exit of the exhaust hood. However, these measured values of CO and NO_x are adopted in the present study because this agrees with a practical application in which emission measurement must be done at the exit of exhaust hood. Therefore, the post-flame zone outside the packed bed will be positively affected by entrainment of the secondary air surrounding the flame and a long residence time for more complete combustion. Almost complete combustion with relatively low CO emission of less than 90 ppm can be achieved because the combustion takes place not only within the packed bed but also at outside of the packed bed with the secondary air entrainment. The trend of CO emission is not significantly changed with *CL* because of the sufficient *PA*. The average minimum and maximum values of CO are 63 ppm at 50 kW and 89 ppm at 35 kW, respectively.

Emission level of NO_x is increased with CL but this is a relatively small in absolute value. However, within the relatively wide experimental range of CL, the maximum value of NO_x does not exceed 81 ppm, which is lower than a standard value employed in various emissions standard for industrial burners. This confirms an outstanding characteristic of the proposed SPMB, which is capable of suppressing the formation of NO_x. According to Sullivan and Kendall [43], it was considered that the thermal NO_x is sensitive to the firing rate and the prompt NO_x is much more sensitive to the theoretical air percent. Thus, at low CL, the prompt NO_x level in this experiment is expected to be a major contribution of the measured value because of relatively rich mixture. The increasing of NO_x at high CL might be caused by thermal NOx because the maximum temperature within the packed bed is increased with CL (see in figure 3.7) and the thermal NO_x will be suppressed if flame temperature is lower than a threshold value of about 1,577°C [43].

3.3.6 Radiative heat loss and output radiation efficiency

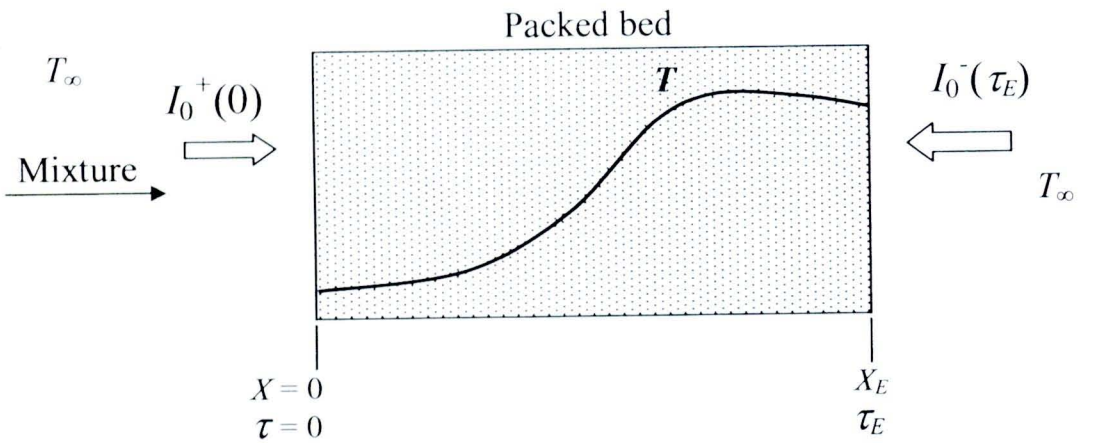

Figure 3.10 Simplified model for computing a radiative heat loss at the inlet and an output radiation efficiency at the exit of the SPMB.

Figure 3.10 shows a simplified model for computing a radiative heat loss at the inlet and an output radiation efficiency at the exit of the SPMB. By assuming that the system is a one-dimensional thermal radiation without scattering, thermal radiation from gas is negligible as compared with the solid, the system is adiabatic and in a local thermodynamics equilibrium, physical properties of solid are constant, and an outside of the SPMB system is exposed to black surrounding maintained at ambient temperature

T_∞ providing incident radiation intensity $I_0^+(0)$ at inlet ($\tau = 0$) and $I_0^-(\tau_E)$ at exit ($\tau = \tau_E$). Then net radiative heat flux at the inlet $q^n(0)$ can be described by Eq. (3.9) [44]:

$$q^n(0) = 2\pi[I^+(0) - I^-(0)] \tag{3.9}$$

Here $I^+(0)$ and $I^-(0)$, respectively, are forward and backward irradiation intensities at the inlet ($\tau = 0$) and are shown by Eqs. (3.10) and (3.11):

$$I^+(0) = I_0^+(0) \tag{3.10}$$

$$I^-(0) = I_0^-(\tau_E)E_3(\tau_E) + \int_0^{\tau_E} I_b[T(\tau')]E_2(\tau')d\tau' \tag{3.11}$$

where τ' is a dummy variable of integration. $I_0^+(0)$ and $I_0^-(\tau_E)$, respectively, are defined by Eq.(3.12):

$$I_0^+(0) = I_0^-(\tau_E) = \frac{\sigma T_\infty^4}{\pi} \tag{3.12}$$

$I_b[T(\tau')]$ in Eq.(3.11) is a black-body radiation intensity as defined by Eq. (3.13):

$$I_b[T(\tau')] = \frac{\sigma T^4}{\pi} \tag{3.13}$$

Here T is a measured porous medium temperature fitted to a continuous function. $E_n(\tau)$ is n^{th} exponential integral function as is defined by Eq.(3.14):

$$E_n(\tau) = \int_0^1 \mu^{n-2}\exp(-\tau/\mu)d\mu \tag{3.14}$$

From Eqs. (3.10) to (3.14), the net radiative heat flux at the inlet $q^n(0)$ can be computed from the measured T from the experiment. Then, radiative heat loss, $\eta_{rad,loss}$, at the SPMB inlet ($\tau = 0$) can be defined by Eq. (3.15):

$$\eta_{rad,loss} = \frac{\text{Net radiation at inlet of SPMB}}{\text{Firingrate}} = \frac{|q^n(0)|A}{CL} \tag{3.15}$$

Here $|q^n(0)|$ is an absolute value of the net radiative heat flux at the inlet of SPMB, and A is its cross-sectional area.

In the same manner as $\eta_{rad,loss}$,ones can obtain output radiation efficiency η_{rad} at the exit of the SPMB ($\tau = \tau_E$) as can be described by Eq. (3.16):

$$\eta_{rad} = \frac{\text{Output radiation at exit of SPMB}}{\text{Firingrate}} = \frac{\left|q^n(\tau_E)\right| A}{CL} \tag{3.16}$$

where

$$q^n(\tau_E) = 2\pi[I^+(\tau_E) - I^-(\tau_E)] \tag{3.17}$$

$$I^+(\tau_E) = I_0^+(0)E_3(\tau_E) + \int_0^{\tau_E} I_b[T(\tau')]E_2(\tau_E - \tau')d\tau' \tag{3.18}$$

$$I^-(\tau_E) = I_0^-(\tau_E) = \frac{\sigma T_\infty^4}{\pi} \tag{3.19}$$

Radiative properties, i.e. optical thickness τ and absorption coefficient κ of the packed bed are estimated from Eqs. (3.20) and (3.21).

$$\tau = \kappa X \tag{3.20}$$

$$\kappa = \varepsilon_{R,eff} \cdot n_p \pi \left(\frac{d}{2}\right)^2 \tag{3.21}$$

where $\varepsilon_{R,eff}$ is an effectiveness emissivity of the packed bed [45] as defined by Eq. (3.22)

$$\varepsilon_{R,eff} = \left\{\frac{(1+\varepsilon_{R,s})}{2} + \frac{(1-\varepsilon_{R,s})}{2}\left[\varepsilon(0.6902 + 0.3803\,\varepsilon_{R,s}) - 1\right]\right\} \pm \varepsilon(1-\varepsilon_{R,s})(0.3451 + 0.1902\varepsilon_{R,s}) \tag{3.22}$$

where $\varepsilon_{R,s} = 0.932$, which is an emissivity of a solid sphere [46].

Radiative heat loss at the burner inlet $\eta_{rad,loss}$ and an output radiation efficiency η_{rad} at the burner exit of the SPMB are shown in figure 3.11. Also η_{rad} of fully premixed porous burners obtained from other studies with a submerged flame [17] and with a surface stabilized flame [47] at different range of CL and equivalence ratio Φ is shown for comparison. Apparently, the surface-stabilized flame [47] at lower CL has shown higher η_{rad} as compared with the submerged flame [17]. However, the surface-stabilized flame [47] shows a sharp decrease in η_{rad} as CL increases and provides good flame stabilization only in a narrow range of CL. In contrast to the surface-stabilized flame, the present SPMB with a partially premixed mixture has shown a relatively high η_{rad}

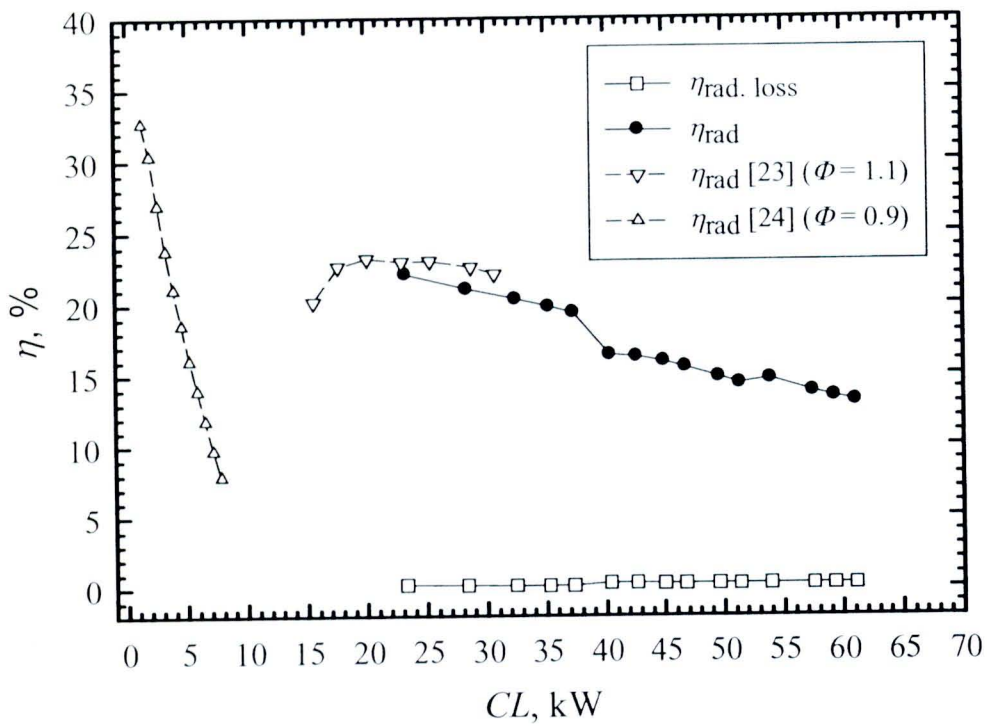

Figure 3.11 Effect of CL on $\eta_{rad,\,loss}$ and η_{rad}.

with good flame stabilization at a wider range of CL. Despite a different CL and Φ studied, the SPMB yields a submerged flame with an intense thermal radiation emitted downstream having an output radiation efficiency η_{rad} as high as 23 percent. The SPMB also shows the same trend as the other submerged flame [17] in terms of maximum η_{rad} and its relationship with the firing rate CL. The SPMB, thus, has the potential to make the best use of η_{rad} of relatively rich mixtures while giving almost zero radiative heat loss at the burner inlet $\eta_{rad,loss}$ and offering low NO_x and low CO emissions. However rich the mixture, it can be completely reacted so long as the temperature of the SPMB is high enough, which is always enhanced by the inherent characteristic of internal heat recirculation by thermal radiation of the submerged flame. Besides, the SPMB is less complicated without complicated devices such as blowers or compressors unit and easier to control as compared with the forced draft burners [17, 47]. This can make the proposed SPMB a new and most promising combustion method for enhancing heat transfer with reducing CO and NO_x emissions from gaseous fuel combustion for clean combustion and highly efficient energy conversion.